IJPAS | INTERNATIONAL JOURNAL PURE AND APPLIED SCIENCES
ISSN:2149-0910

Vol. 10(2); 604-622 (2024)
DOI: 10.29132/ijpas.1569593

Research Article

The Ptcdi-C8/P-Si Heterojunction Diode: Its Construction and Electrical Characterization

Murat ERDAL [1], Cihat ÖZAYDIN [2,*]

Received: 18.10.2024

Accepted: 25.12.2024

[1] Batman University, Faculty of Art&Science, Department of Physics, Batman Türkiye; physicist.721@gmail.com
[2] Batman University, Faculty of Engineering and Architecture, Department of Computer Engineering, Batman, Türkiye; cihat.ozaydin@batman.edu.tr
* Corresponding author

Abstract: In this study, an Al/PTCDI-C8/p-Si organic-inorganic (OI) heterojunction diode (C1) was fabricated by depositing a PTCDI-C8 thin film onto p-Si using the spin coating method. Likewise, a conventional Al/p-Si metal-semiconductor (MS) diode (C0) was fabricated without the use of an interlayer. I-V and C-V measurements of the C0 and C1 diodes were taken in the dark and at room temperature. The rectifying properties of both diodes were good. From the I–V characteristics, the ideality factor, barrier height, and series resistance of the C1 diode were determined to be 2.1, 0.74 eV, and 248 kΩ, respectively. The BH value obtained for the C1 heterojunction is higher than the value obtained for the conventional C0 diode. The electrical parameters of both the C1 and C0 diodes, particularly the series resistance, were recalculated using Cheungs and Norde methods. At room temperature, the C-V measurements of the diodes were carried out at various frequencies. From the evaluation of the C-V characteristics, the diffusion potential (V_d), barrier height ($\Phi_{b(C-V)}$), and free carrier density (N_A) of both diodes were calculated. Additionally, the device's photovoltaic parameters were measured under illumination conditions. The C1 heterojunction shows a photodiode behavior with the obtained photovoltaic parameters Voc and Isc.

Keywords: Heterojunction diode; PTCDI-C8; thin films; electrical characterization

Ptcdi-C8/P-Si Heterojunction Diyot: Yapısı ve Elektriksel Karakterizasyonu

Özet: Bu çalışmada, p-Si üzerine spin kaplama yöntemi kullanılarak PTCDI-C8 ince filmi büyütülerek Al/PTCDI-C8/p-Si organik-inorganik (OI) heteroeklem diyotu (C1) üretildi. Benzer şekilde, geleneksel Al/p-Si metal-yarı iletken (MS) diyotu (C0) ara katman kullanılmadan üretildi. C0 ve C1 diyotların I-V ve C-V ölçümleri karanlıkta ve oda sıcaklığında alındı. Her iki diyot da iyi doğrultucu özellikler gösterdi. I-V karakteristiklerinden, C1 diyotunun idealite faktörü, bariyer yüksekliği ve seri direnci sırasıyla 2,1, 0,74 eV ve 248 kΩ olarak belirlendi. C1 heterojunsiyonu için elde edilen BH değerinin, geleneksel C0 diyot için elde edilen değerden daha yüksek olduğu gözlendi. Hem C1 hem de C0 diyotların elektriksel parametreleri, özellikle seri direnç, Cheungs ve Norde yöntemleri kullanılarak yeniden hesaplandı. Oda sıcaklığında, diyotların C-V ölçümleri farklı frekanslarda gerçekleştirildi. C-V karakteristiklerinden, her iki diyotun difüzyon potansiyeli (V_d), bariyer yüksekliği (Φb(C-V)) ve serbest taşıyıcı yoğunluğu (N_A) hesaplandı. Ayrıca, C1'in fotovoltaik

parametreleri aydınlatma koşulları altında ölçüldü. C1 heteroeklemi, elde edilen fotovoltaik parametreler Voc ve Isc ile bir fotodiyot davranışı göstermektedir.

Anahtar Kelimeler: Heteroeklem diyot; PTCDI-C8; ince film; elektriksel karakterizasyon

1. Introduction

Organic molecules are of great interest due to their unique optical and structural properties and are widely utilized in various fields [1]. Organic semiconductor compounds are widely used in many optoelectronic devices and applications such as solar cells [2-4], transistors (OFET) [5-7], diodes [8-10], sensors [11-12] and detectors [13-14]. Among organic semiconductor compounds, perylene derivative PTCDI (Perylene-3,4,9,10-tetracarboxylic diimide) is shown as a promising small molecule organic semiconductor [1, 15, 16, 17]. PTCDI molecules are n-type materials and have good thermal and photostability properties [18]. There are different Ptcdi derivatives. The electron-accepting photoactive compound N,N'-dioctyl-3,4:9,10-perylene tetracarboxylic diimide (PTCDI-C8) has an aromatic core and two opposing alkyl chains, each with eight C atoms [19, 20]. Fig. 1 shows the chemical structure of PTCDI-C8. Perylene bisimides; owing to the planar core's π-electron system, they also want to bond with other atoms, making them an excellent candidate in relation to organic electrical devices and with electron mobility up to 1.7 cm^2. Additionally, PTCDI-C8 exhibits strong absorption in the visible spectrum's blueshift region (400–600 nm), with peaks at 488 nm, 523 nm, and 567 nm, making it an attractive material for use as an acceptor material in organic photovoltaic devices [21].

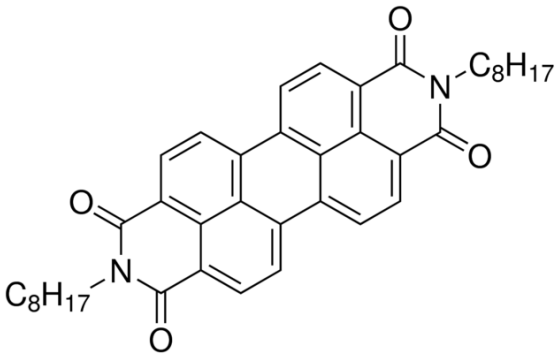

Figure 1. Chemical structure of PTCDI-C8

In the context of semiconductor devices, the metal-semiconductor (MS) contact has a fundamental and predominant function. MS contacts are an important field of study for optoelectronic applications as they form the basis of semiconductor device structures [22]. There is a significant influence of the interface barrier properties on the characteristics of MS contacts. It is possible to modify the electrical properties of the MS contact if a suitable organic semiconductor intermediate layer is placed between the metal and the semiconductor [23]. To date, there are many scientists who have examined the electrical characteristics of the organic based Schottky barrier diodes (SBDs) utilizing various organic compounds. For instance, in one of the first studies on this subject, according to Forrest et al. [24], metal-insulator-semiconductor (MIS) connections were created by sublimating non-polymeric organic films onto a semiconductor wafer, followed by the evaporation of several metals. The ideality factor and barrier height (BH) were then measured. Campbell et al. [25] have placed an organic film at the MS interface. They reported that the effective BH could be changed in this way. Huang et al. [26] reported the electrical parameters of the Al/Alq3/p-Si diode by measuring the current and capacitance versus voltage. The diode's ideality factor and BH values were found to be 1.53 and 0.78 eV, respectively, and it was reported that the BH of the Al/Alq3/p-Si heterojunction was higher than that of the standard

Al/p-Si diode (0.58 eV). Thus, they discovered that the diode's carrier transport at the contact interface is regulated by the organic Alq3 layer.

There are many experimental studies on the effect of organic semiconductor materials such as perylene derivatives, perylene tetracarboxylic dianhydride (PTCDA) and PTCDI, in optoelectronic device applications [27]. To be utilized in these kinds of applications, a device's characteristic properties must be understood. In this paper, a thin film of organic semiconductor material (PTCDI-C8) grown by the sol-gel method was used as an interface layer between Al and p-Si in a conventional SBD. The PTCDI-C8 is an organic material with high mobility and n-type semiconductor properties, which is very suitable for electronic and optoelectronic devices. This study explores the potential of Ptcdi-C8 as an organic semiconductor in interfacial Schottky diode applications, highlighting its capacity to provide innovative solutions in the field of organic electronics. The findings hold substantial importance for advancing both fundamental scientific understanding and cutting-edge technological applications. The Al/PTCDI-C8/p-Si heterojunction is designed to improve the electrical and photoelectric properties of the traditional diode. By examining I-V (current to voltage) and C-V (capacitance to voltage) characteristics, the PTCDI-C8/p-Si heterojunction was electrically characterized. Diode's series resistor (R_S) value, which gives us information about the interface properties, was calculated by Norde and Cheung's methods. I-V characteristics under illumination have also been used to study the photovoltaic properties.

2. Experimental

In this study, PTCDI-C8 was used and purchased from Sigma Aldrich. A single-sided polished p-type silicon wafer (p-Si) with 400 µm thickness, [100] orientation and acceptor concentration of 1.04×10^{19} cm^{-3} (purchased from MTI Corporation, USA) was used as inorganic semiconductor substrate. For chemical cleaning, the wafer was first dipped in boiling 3-chloroethylene to degrease and washed with ultrasonic vibration in acetone and methanol for 5 minutes. Then, the semiconductor was etched by immersion in a H_2O/HF (10:1) solution for 30 seconds to remove the natural oxide layer on its surface. The Si wafer was washed in Deionized (DI) (18 MΩ) water following each procedure. To create ohmic contact, metal (Al) with 110 nm thickness and 99.99% purity was evaporated in high vacuum (3×10^{-6}) on the unpolished side of the Si substrate. In a N_2 gas environment, thermal annealing was carried out for three minutes at 570 °C to provide a low resistance back contact. The oxide layer on the p-Si wafer surface was removed with 10% HF solution, as mentioned above. and rinsed for 60 seconds in 18 M DI water and dried before forming a PTCDI-C8 film layer on the wafer. Chloroform was used as a solvent for PTCDI-C8 solution. Spin coating was used to create an organic PTCDI-C8 thin film on the p-Si substrate. The spin coating process was carried out with 1200 rpm rotation speed, 30s time and 10 repetitions of the process. After the formation of the Al/PTCDI-C8/p-Si structure, Al metal was thermally evaporated onto the PTCDI-C8 thin film using a shadow mask to form the top contact under a high vacuum condition (10^{-6} Torr). As a comparison, an interlayer-free Al/p-Si (C0) diode was also created. The schematic representation of the manufactured Al/PTCDI-C8/p-Si (C1) heterojunction is shown in Figure 2.

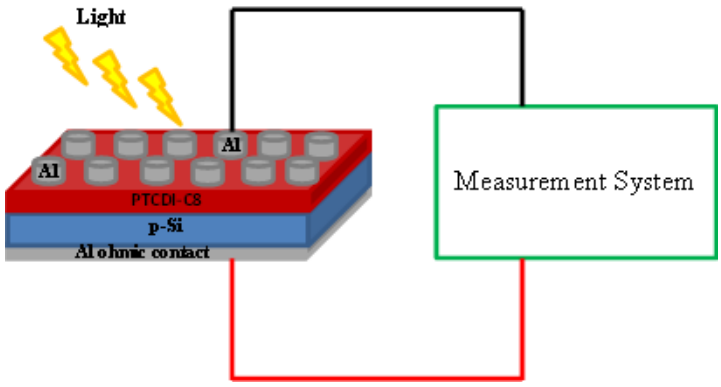

Figure 2. Schematic representation of the Al/PTCDI-C8/p-Si heterojunction diode as constructed.

At room temperature and in the dark, measurements of I-V and C-V were made using the 4200-SCS (Keithley Institute, USA). I-V measurements under light were performed with a Science-tech-SF150 (Sciencetech inc., London) sun simulator with an AM1.5filter to study photovoltaic properties.

3. Results and Discussion

3.1. Analysing the I-V Properties in the Dark

Critical metrics in the electrical characterization and quality assessment of a SBD are the reverse saturation current, ideality factor, and Schottky BH [22]. The semi-log plot of forward (Fwd)-reverse (Rev) I–V characteristics of the C0 diode and C1 heterojunction diode in darkness are shown in Fig.3.

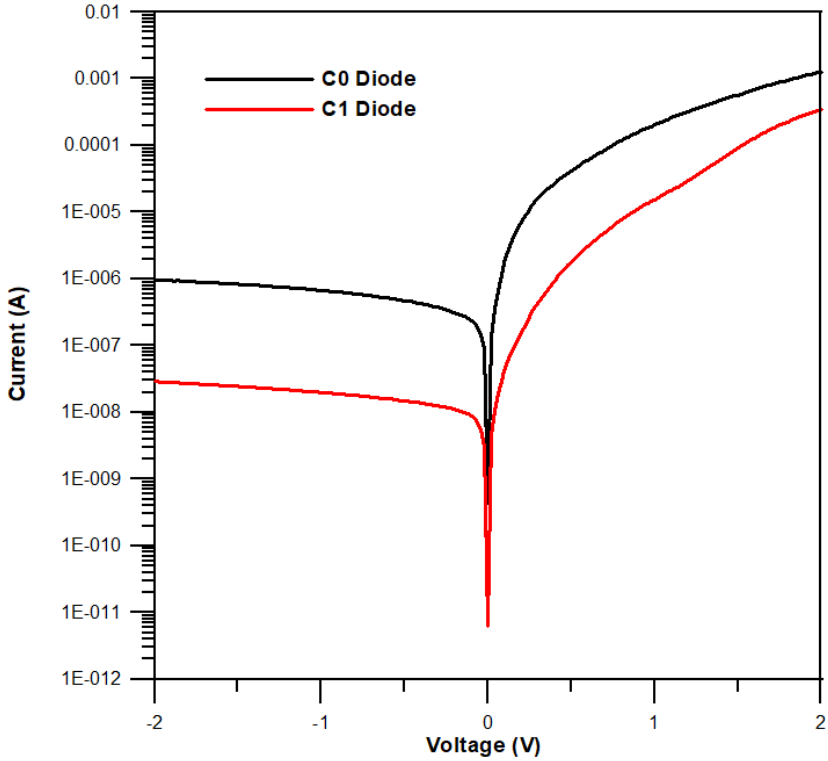

Figure 3. Semilogarithmic I–V characteristics of the C0 diode and C1 heterojunction diode.

The diodes have good rectification properties, as shown in Fig 3. For rectifying contacts, the ideality factor (n) is determined as in the Eq. (1).

$$\boldsymbol{n = \frac{q}{kT}\frac{dV}{d(lnI)}} \quad (\mathbf{1})$$

where, q is the charge, k is the Boltzman constant, T is the temperature, V is the applied voltage, and the diode's current is represented by I. The ideality factor values of the C0 diode and the C1 heterojunction diode were determined from the slope of the linear part of the forward current region of the semi-logarithmic I-V characteristic and were found to be 1.58 and 2.1, respectively. These n values are slightly higher than unity. The unique interface structure, in particular the interface dipoles at the interface brought on by series resistance, and manufacturing defects are the secondary factors responsible for very high n values. According to another research [28], the high n values are attributed to the broad distribution of low Schottky barrier patches, which result from lateral barrier inhomogeneity [28, 29]. The dark current for C0 and C1 diodes can be expressed by the non-ideal diode form in Eq. (2)[30].

$$\boldsymbol{I = I_0\left[exp\left(\frac{e(V - IR_s)}{nkT}\right) - 1\right]} \quad (2)$$

Here, I_0 is the diode's saturation current and is given as:

$$\boldsymbol{I_0 = AA^*T^2 exp\left(-\frac{q\phi_{b0}}{kT}\right)} \quad (3)$$

where A is the diode's contact area, Richardson Constant, A^*, for p-Si is 32 A/cm^{2}K^2, and ϕ_{b0} is the effective Schottky BH at zero bias. The reverse saturation current, I_0 is obtained by extrapolating the linear region of the Fwd I–V curves to the zero applied voltage. The reverse saturation currents at room temperature were determined as 1.44x10^{-7} A and 6.41x10^{-9} A for C0 and C1 diodes, respectively. It is understood that the use of the PTCDI-C8 interlayer in the Al/p-Si structure makes a significant change in the saturation current. Experimental ϕ_{b0} values were calculated from the I and V characteristics from the following relationship.

$$\boldsymbol{\phi_{b0} = \frac{kT}{q}\ln\left(\frac{AA^*T^2}{I_0}\right)} \quad (4)$$

From Equation (4), experimental ϕ_{b0} values for C0 and C1 diodes in the dark were obtained as 0.66 eV and 0.74 eV, respectively. In the literature, there have been some studies showing that the BH is modified by the use of organic thin films as an interlayer in MS contacts. Recently, Marıl [31] published an article about the organic interlayer Al/PVO-Cu2Te/p-Si diode with a barrier height of 0.692 eV and an ideality factor of 1.85. The obtained BH value of this diode was reported to be bigger than conventional Al/p-Si (ϕ_{b0}=0.576 eV) and evaluated that the organic substrate improved the performance of MS diode by increasing BH. In another study, Karadeniz et al. [32] found the BH values of Al/p-Si and Al/rubrene/p-Si diodes to be 0.649 and 0.771. They attributed the increase in BH to the rubrene layer might significantly alter the metal's work function and the electron susceptibility of the semiconductor, whereas the organic layer gave an increase of 0.122 eV. Imer et al. [33] fabricated the Sn/MY/p-Si and Sn/p-Si diodes, and obtained the BH value of the Sn/MY/p-Si diode bigger than the Sn/p-Si device. They explained this increase in terms of interfacial states charges and the use of an organic interlayer to passivate unsaturated bonds on the surface of the Si substrate. Furthermore, results from earlier studies have demonstrated that the electrical conductivity of the organic semiconductor to be used in the fabrication of the MS device, the organic film's preparation method, and the thickness of the film all have a substantial impact on the device's electronic parameters and performance [34]. Based on the experimental results we obtained and those mentioned above, we evaluate that the conventional MS diode can be designed to exhibit the desired properties with the appropriate organic molecule selection.

Another important parameter for the Schottky barrier diodes (SBDs) is the series resistance (R_S). At relatively high voltages, the fwd bias I–V plots of the diode deviate from linearity due to R_S. Here, the well-known Cheungs and Norde methods are used to calculate the Rs values. According to Cheung and Cheung [35], the R_S values of the SBDs can be calculated from the following functions:

$$\frac{dV}{d(lnI)} = IR_s + n\frac{kT}{q} \quad (5)$$

$$H(I) = n\phi_b + IR_s \quad (6)$$

H(I)-I and dV/dln(I)-I graphs of C0 and C1diodes derived from Equations (5) and (6) are shown in Figure 4 and Figure 5, respectively.

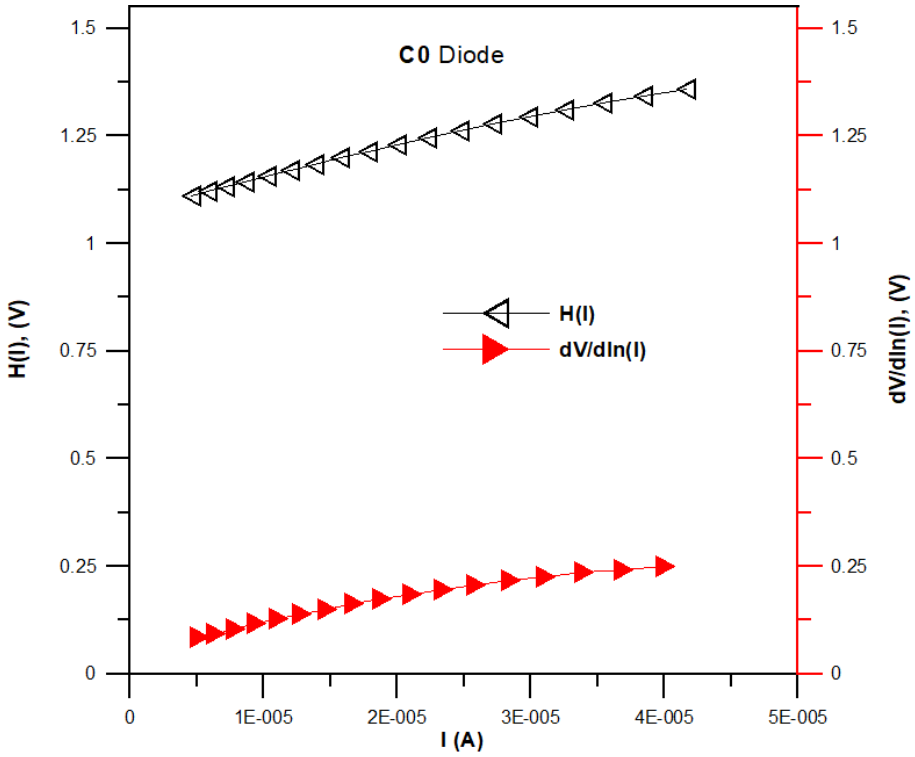

Figure 4. H(I)-(I) and dV/d(lnI)-I graph of C0 reference diode.

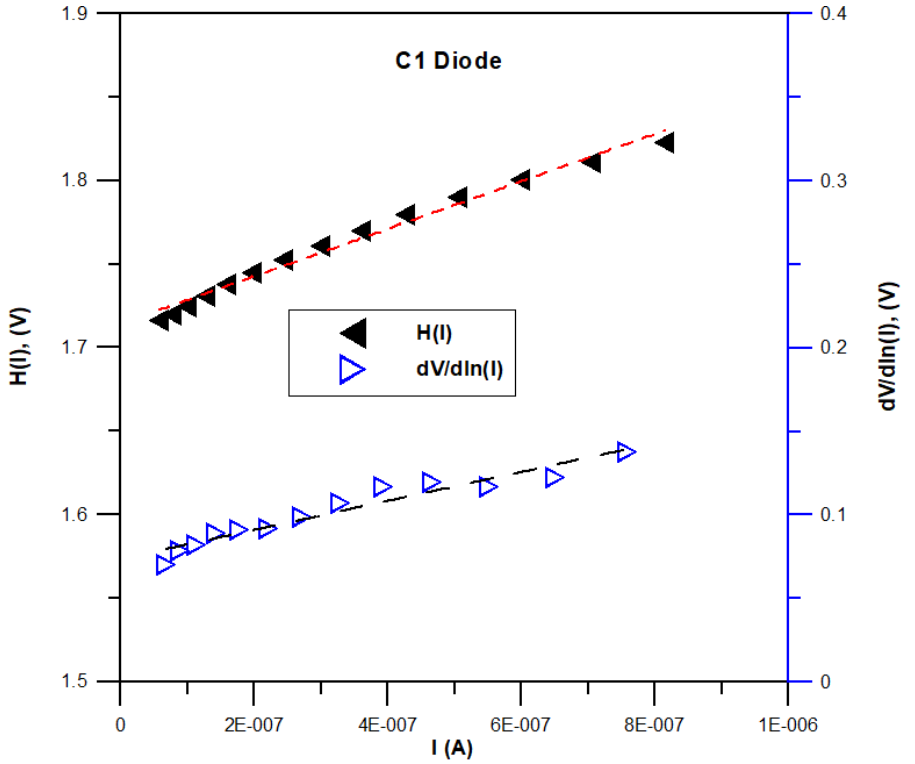

Figure 5. H(I)-(I) and dV/d(lnI)-I graph of C1 diode.

Both of these graphs will be linear. The series resistance (*Rs*) is obtained from the slope of the dV/dln(I)-I plot, and the ideality factor is obtained from intersection of the y-axis. Similarly, the *Rs* is obtained from the slope of the H(I)-I plot and the barrier height is obtained from intersection of the

y-axis. Series resistance and other parameters obtained from Cheungs' functions for C1 and conventional C0 diodes are given in Table 1.

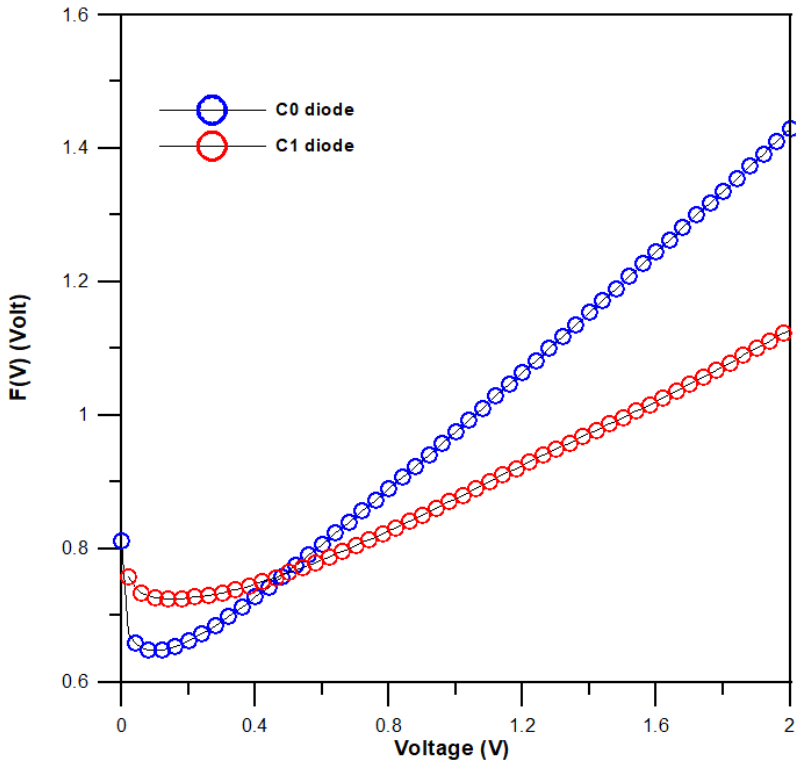

Figure 6. F(V)-V (Norde) plots of C0 (blue) and C1 (red) diodes.

The greater series resistance of the C1 heterojunction diode than the C0 diode is attributed to the presence of the interlayer, the presence of interfacial states, and the natural/accumulated interlayer barrier inhomogeneity at the metal-semiconductor interface [29, 31]. In addition to this, ϕ_b values obtained from both TE and Cheung methods for both diodes were obtained quite consistently. The Norde method is another recommended way to calculate the *Rs* value [36]. The Norde function modified by Bohlin [37] for SBDs with high series resistance and ideality factor is defined as follows.

$$F(V) = \frac{V}{\gamma} - \frac{kT}{q}\ln\left(\frac{I(V)}{AA^{*}T^{2}}\right) \tag{7}$$

Here γ is an integer constant larger than *n* and *I(V)* is the value corresponding to *V* voltage in current-voltage data. In Figure 6, F(V)-V graphs for diodes C0 and C1 are displayed. Once the minimum of the F-V graph has been found, the barrier height value of the diodes can be determined using Eq. 8.

$$\phi_b = F(V_0) + \frac{V_0}{\gamma} - \frac{kT}{q} \tag{8}$$

where $F(V_0)$ is the min. value of *F(V)* and V_0 is its matching voltage value. According to the Norde method, *Rs* of the diode is calculated via the following relationship:

$$R_s = \frac{kT(\gamma - n)}{qI_0} \tag{9}$$

Here I_0 is the forward bias current at V_0. Parameters and values used for C1 and C0 diodes in Norde functions are V_0: 0.14-0.1 V, $F(V_0)$: 0.725-0.648, γ =3-2, I_0:1.575x10, respectively It was taken as

-6-7.64x10-8 A. The *Rs* and BH values calculated from Norde functions were obtained as ϕ_b: 0.787-0.672 eV and *Rs*: 248-6.12 kΩ, respectively, and are shown in Table 1. The values derived from the Cheungs functions are lower than the values derived from the Norde functions in terms of *Rs*. This is because; the Norde function is generally valid for ideal SBD. In addition, Norde functions are applied to all fwd bias I–V characteristics, while Cheungs functions are applied only to the relatively high voltage non-linear region of fwd bias I–V characteristics [38].

Table 1. *Electronic parameters of C0 and C1 diodes.*

	Cheungs Functions				**Experimental**		**Norde Functions**	
	dV/d(lnI)-I		*H(I)-I*		**ln I–V**		*F(V)-V*	
Sample	*Rs (kΩ)*	*n*	*Rs (kΩ)*	$\phi_b\ (eV)$	*n*	$\phi_b\ (eV)$	*Rs (kΩ)*	$\phi_b\ (eV)$
Al/p-Si (C0)	4.82	2.88	6.78	0.679	1.58	0.662	6.12	0.672
Al/PTCDI-C8/ p-Si (C1)	86	2.87	142	0.758	2.10	0.742	248	0.787

3.2. Analysis of the Capacitance-Voltage Characteristics in the Dark

Measurements of capacitance-voltage (C-V) are one of the crucial methods used to determine the interfacial state densities, giving information about the quality of MIS diodes. The C–V characteristics of C0 and C1diodes were measured between 10 kHz and 1 MHz in the dark and at room conditions. The C-V graphs of diodes C0 and C1 are shown in Figure 7 and Figure 8 respectively.

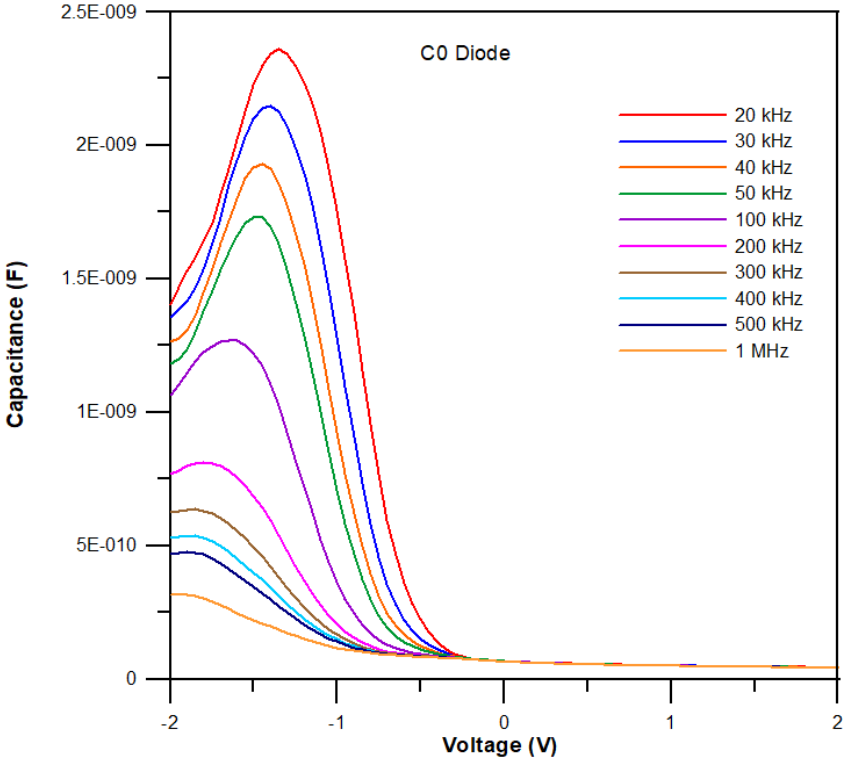

Figure 7. C-V characteristics of C0 diode from 20kHz to 1MHz.

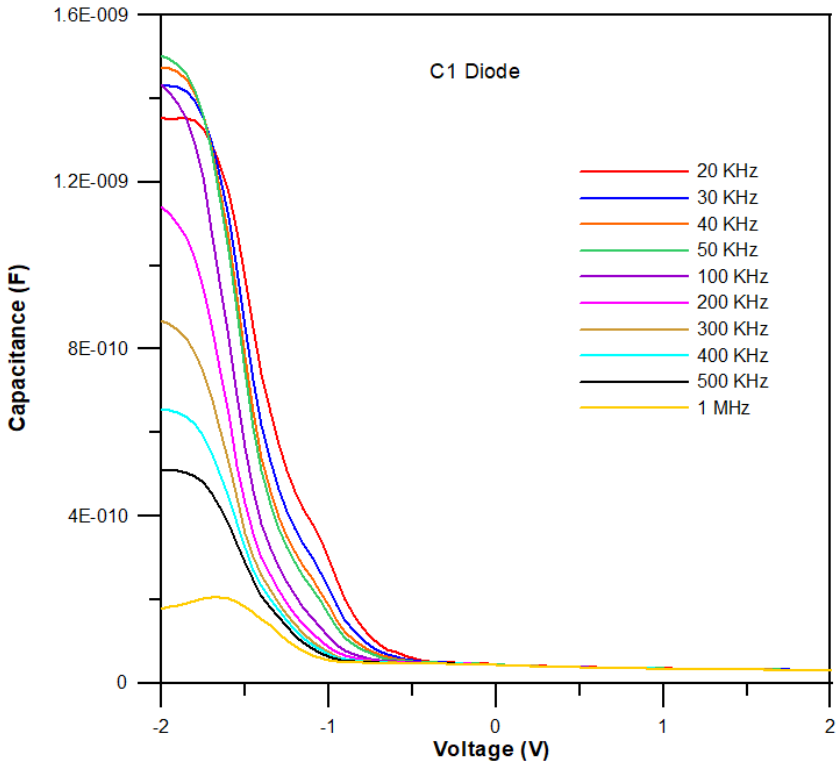

Figure 8. C-V characteristics of C1 diode from 10kHz to 1MHz.

In general, the measured capacitance for the rectifier contact depends on the rev bias voltage and its frequency [39]. As seen in Figures 7 and 8, as the frequency increases, the capacitance value decreases at reverse bias voltages and disappears at forward bias voltages. This is because the interface states do not significantly contribute to the capacitance at high frequencies because they are unable to follow the alternate current (AC) signal [39]. The relationship between capacitance and voltage for Schottky diodes is expressed as [40]:

$$C^{-2} = \frac{2(V_d + V)}{qA^2\varepsilon_s N_a} \tag{10}$$

where, A is the diode's effective area, N_a is the carrier concentration, ε_s is dielectric constant of the semiconductor ($\varepsilon_s = 11.8\varepsilon_0$), and V_d represents the diffusion potential with no bias. The BH value of the diodes from C-V can be determined from the relationship:

$$\phi_b(C - V) = q\left(c_2 V_d + V_p\right) \tag{11}$$

where c_2 is a coefficient equal to n^{-1}, Vp is the potential difference between the Fermi level in the neutral region of p-Si and the top of the valence band and is calculated as:

$$V_p = kTln\left(\frac{N_v}{N_a}\right) \tag{12}$$

where N_v is the density of effective states and for p-Si this value is $N_v = 1.04 \cdot 10^{19}$ cm^{-3}. The C^{-2} –V graphs ploted from C-V measurements of C0 and C1 diodes at 500 kHz are shown in Fig. 9 and 10, respectively.

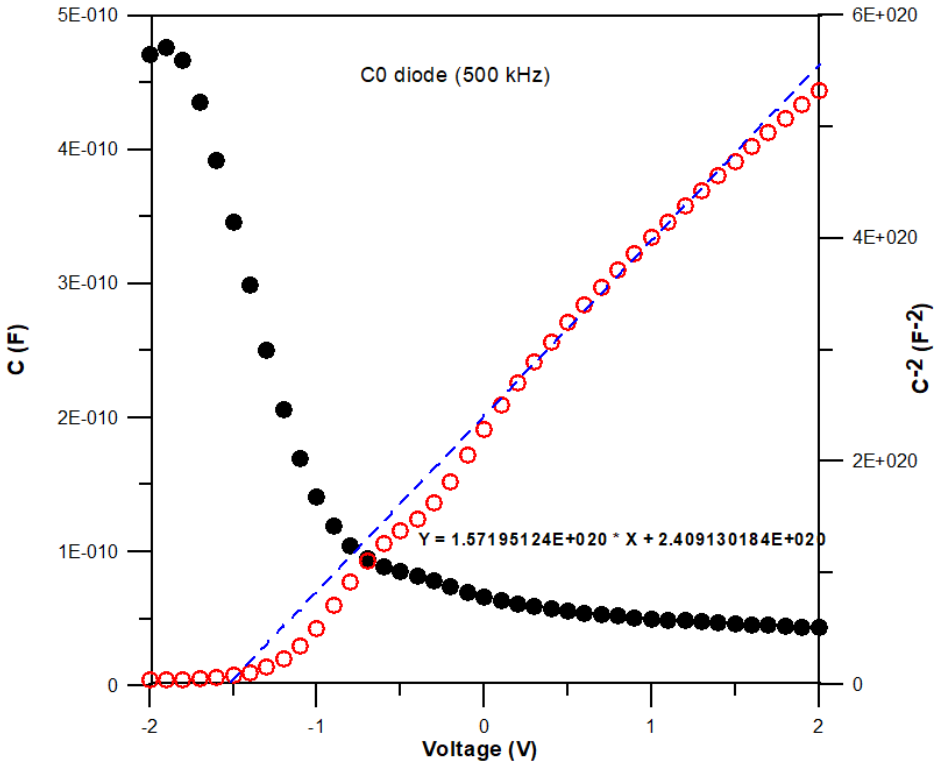

Figure 9. The C-V (black circles) and C^2-V (red rings) graphs of C0 diode at 500kHz.

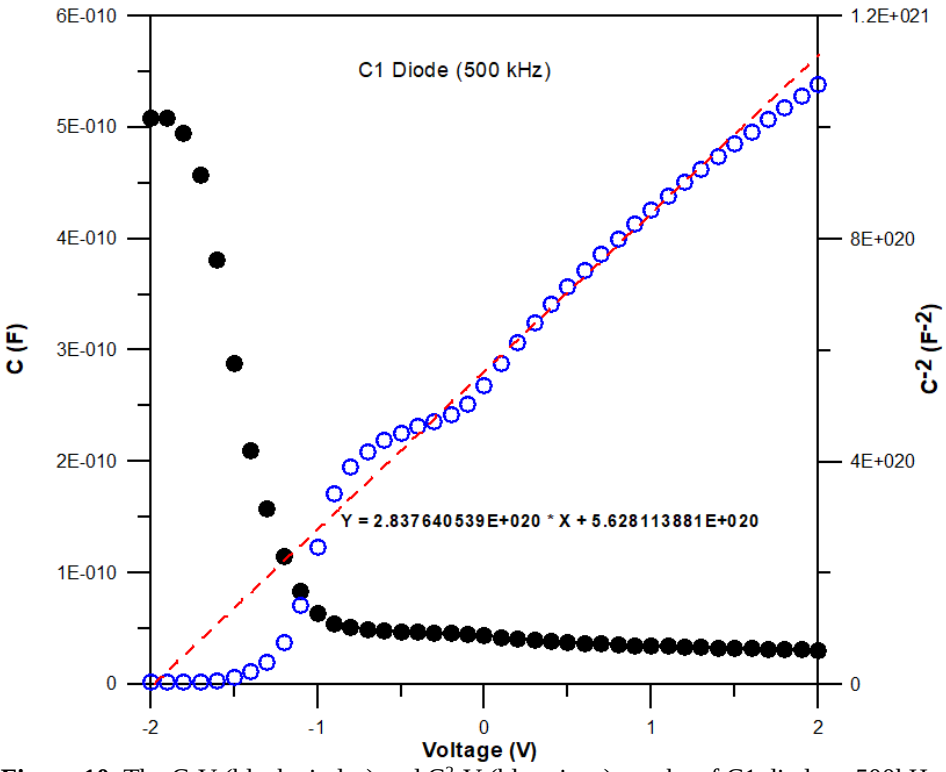

Figure 10. The C-V (black circles) and C^2-V (blue rings) graphs of C1 diode at 500kHz.

N_a is obtained by measuring the linear portion of the C^{-2}–V graph's slope and V_d is obtained from the intersection of the C^{-2} axis at zero bias. There BH values of C0 and C1 diodes derived from C-V characteristics were determined to be 0.765 eV and 0.938 eV, respectively. The parameters of C0 and C1 diodes obtained from the C-V are given in Table 2. The ϕ_b values derived from the C–V are larger

than the ϕ_b values derived from the I–V. Excess capacitance and BH inhomogeneities could be the cause of the discrepancy between the BHs measured from C–V and I–V [41]. The BH derived from C-V approach is usually larger because it is not affected by possible variations on length scales less than the area-charge width that the C-V method averages over the whole area for [32,33,34].

Table 2. *The parameters of C0 and C1 diodes obtained from the C-V characteristics*

Sample	$\boldsymbol{\phi_b}$ **(C − V) (eV)**	$\boldsymbol{N_a}$ **(cm^{-3})**	$\boldsymbol{V_d}$ **(V)**	$\boldsymbol{V_p}$ **(V)**
Al/p-Si (C0)	0.765	1.23x10^{15}	1.533	0.233
Al/PTCDI-C8/p-Si (C1)	0.938	6.85x10^{14}	1.983	0.247

Conductivity-voltage measurements are also important in terms of showing series resistance. Conductivity-voltage (G–V) properties of C0 and C1 diodes were measured between 10 kHz and 1 MHz in the dark and at room conditions. The G-V graphs of C0 and C1 diodes are shown in figures 11 and 12, respectively.

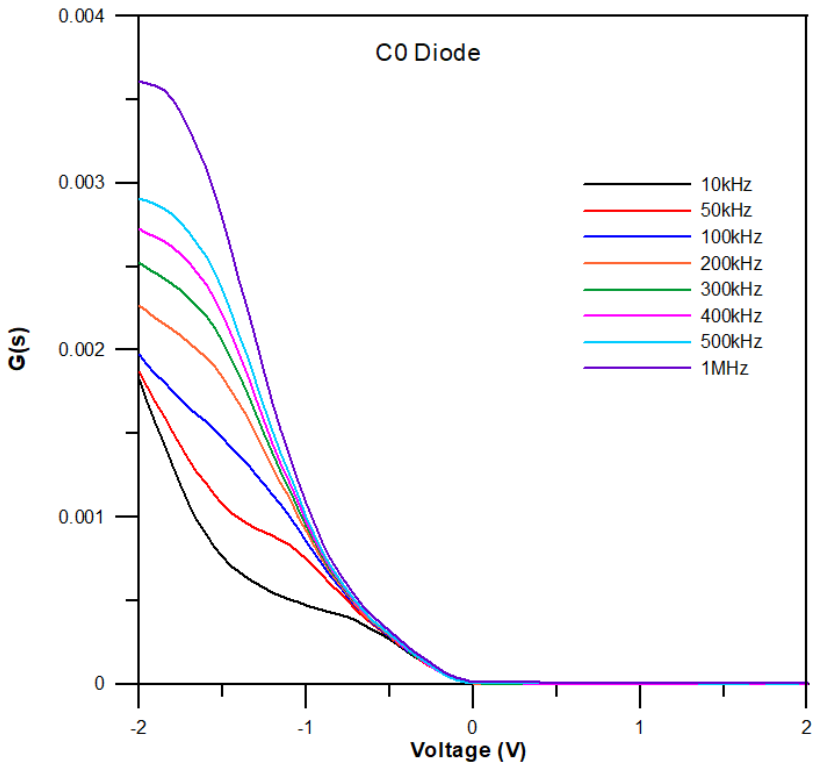

Figure 11. Conductivity-voltage (G–V) characteristics of C0 diode.

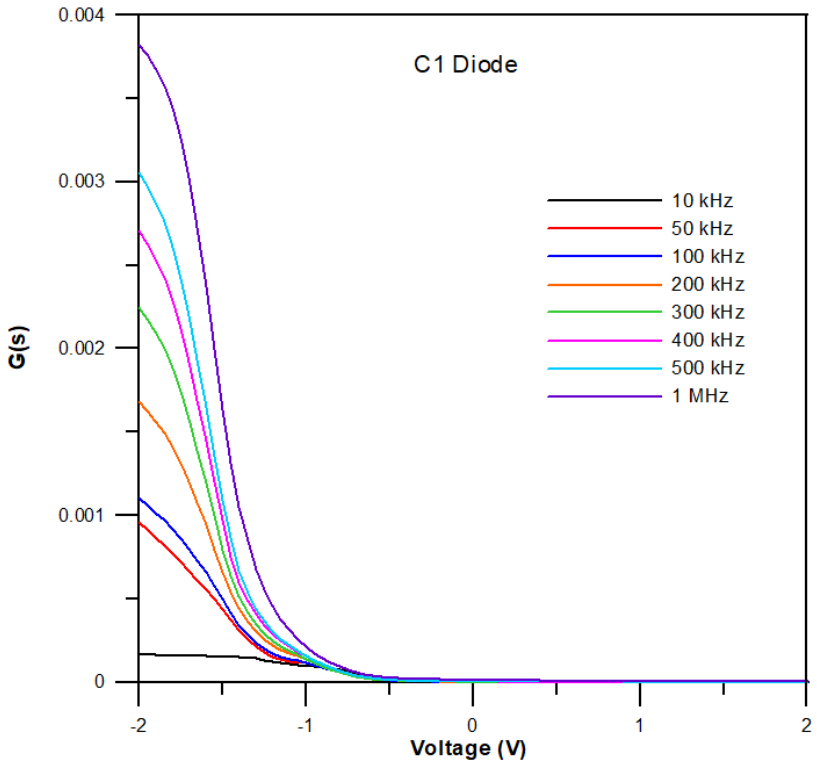

Figure 12. Conductivity-voltage (G–V) characteristics of C1 diode.

In Figures 11 and 12, it is seen that the AC conductivity increased with increasing frequency. This can be explained by attributing the existence of the Schottky barrier and the effect of the series resistance. The frequency-dependent R_S can be obtained from the C-V and G-V measurements with the following equation:

$$R_S = \frac{G_m}{G_m^2 + (wC_m)^2} \tag{13}$$

Where G_m and C_m represent the measured capacitance and conductance, respectively and w is the angular frequency. R_S -V plots of C0 and C1 diodes at different frequencies (10 kHz-1 MHz) are shown in figures 13 and 14. As can be seen in Figs. 13 and 14, the R_S values are quite high and these high R_S values have a great influence on the non-ideal behavior of the diode.

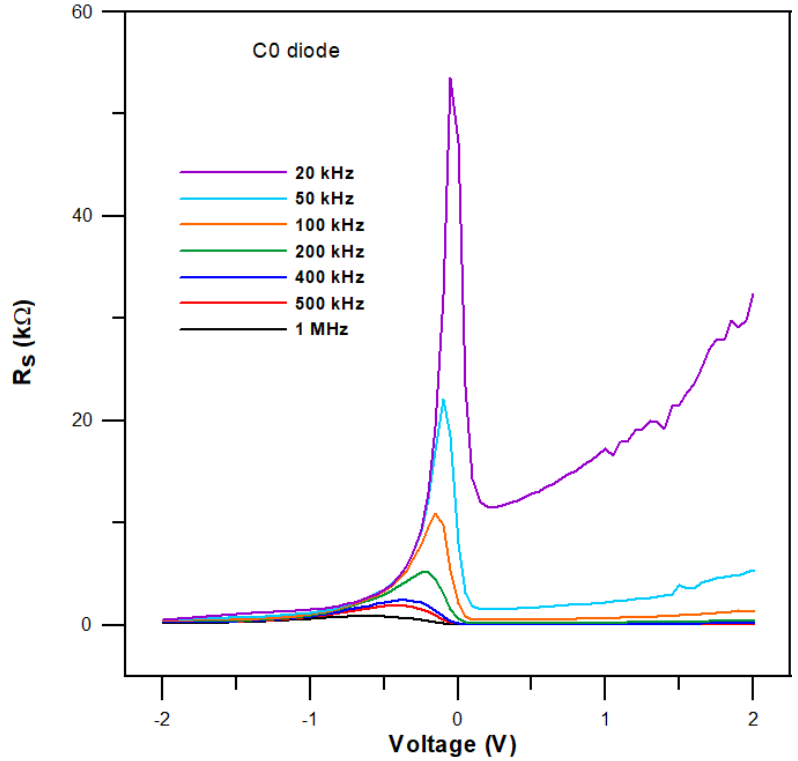

Figure 13. The R_S -V plots of C0 at different frequencies (20 kHz-1 MHz).

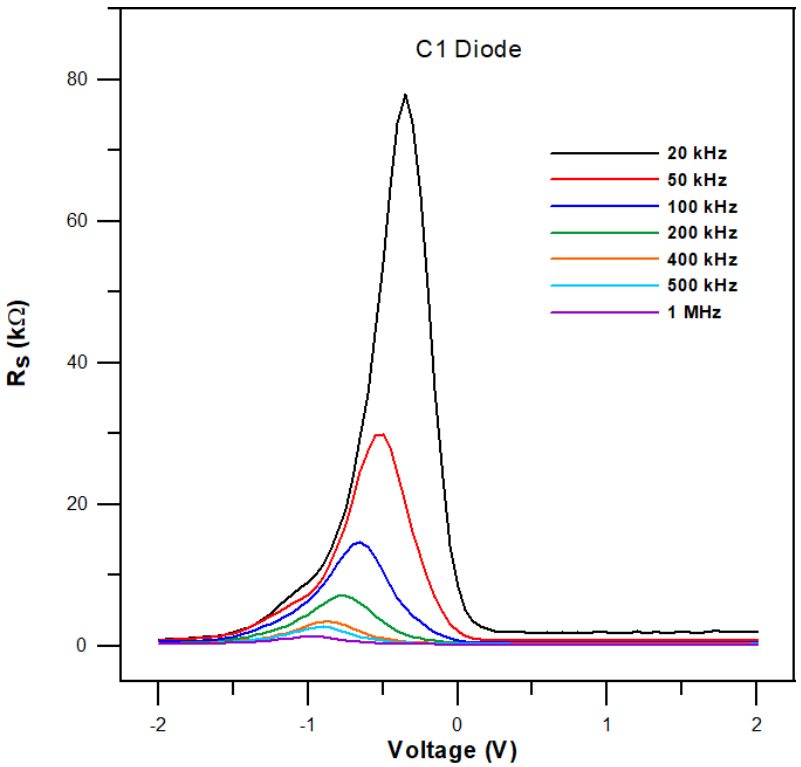

Figure 14. The R_S -V plots of C1 at different frequencies (10 kHz-1 MHz).

Besides, as also seen in R_S -V plots, R_S provides a peak in the rev. bias region. With decreasing frequency, the peak position of the R_S moves to the higher reverse bias area, and at high enough frequencies, it nearly vanishes. The change in peak intensity indicates the interface states following the

AC. However, the peak disappears after 500 kHz for C0 and C1 diodes, respectively, indicating that the interface states cannot follow AC [42].

3.3. Photovoltaic characteristics

The semi-logarithmic ln(I)-V graphs of C0 and C1 diodes under light are (100 mW/cm^2) shown in Figures 15 and 16, respectively.

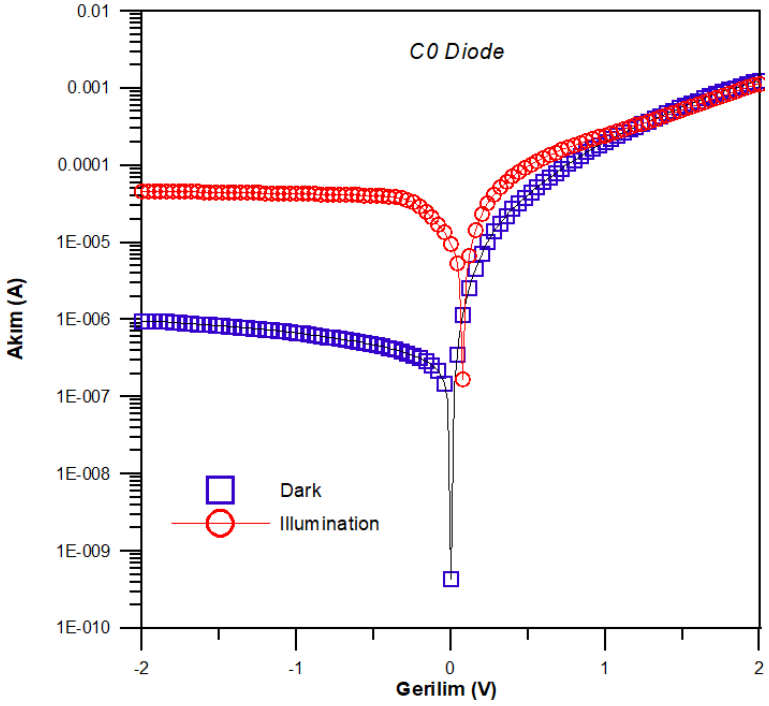

Figure 15. The semi-log I-V plots of C0 diode under dark and light (100 mW/cm^2).

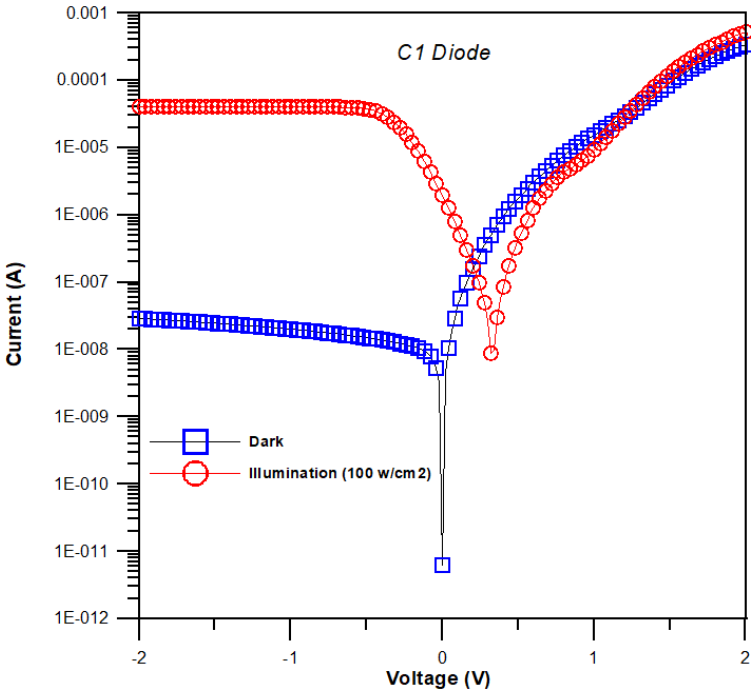

Figure 16. The semi-log I-V plots of C1 diode under dark and light (100 mW/cm^2).

The open-circuit voltage V_{OC}: 80 mV and the short-circuit current I_{SC}: 9.66 µA were obtained for the **C0** diode from the I-V feature under the light. The photosensitivity value for the heterojunction was defined as the rate of photo current to dark current (Iph/Idark) [39, 43]. The C0 diode exhibits a photosensitivity of 48.2 under 100 mW/cm^2 light illumination at -2V. The V_{OC}: 320 mV and the I_{SC}: 1.91 µA were obtained from the I-V feature of C1 under light illumination. The C1 heterojunction diode exhibits a photosensitivity of 1418.7 under 100 mW/cm^2 light illumination at -2V. It has been noted that illumination significantly increases the photocurrent in the device's reverse bias. The photovoltaic effect in the heterojunction can be explained as follows; PTCDI-C8 organic semiconductor absorbs light and charge is transferred to Si, giving off photocarriers produced in this generation OI interface and in turn countercurrent increases efficiency significantly [44]. The photovoltaic properties show that the light absorption by the active layer generates carrier that contribute to the photocurrent due to the production of excitons and their subsequent dissociation into the free charge carriers at the barrier, i.e., PTCDI-C8/p-Si interface [39].

4. CONCLUSIONS

The electrical properties of C0 reference diode and C1 heterojunction diode were investigated with I-V and C-V characteristics. For the C0 reference diode, the experimental BH ϕ_b =0.662 eV and ideality factor *n*= 1.58 were calculated from the data obtained from the I-V characteristic under dark and at room temperature. The saturation current (I_0) of the diode was obtained as 1.44x10^{-7} A. Under the same conditions, the experimental BH, *n* and I_0 values of the PTCDI-C8 thin-film interlayer diode were obtained as 0.742 eV, 2.1, and 6.41x10^{-9}, respectively. The fact that these diode parameters obtained from C0 were different from those of C1 indicates that the PTCDI-C8 organic thin layer modifies the BH due to the shift in the metal's work function and the semiconductor's electron affinity. It is also evidence of the existence of a thin-film interlayer. In a recent study, Tezcan et al. [45] found the ideality factor and barrier height of the Al/PyMIs/p-Si/Al diode to be 2.51 and 0.77 eV, respectively. In another recent study, Şahin et al. [46] found the ideality factor and barrier height of newly synthesized π-conjugated BODIPY dye based Au/n-Si diode to be 2.66 and 0.907 eV in the dark, respectively. A great deal of research has been done using various organic interlayers in Al-pSi diode [45–50]. The contact parameters of Al/PTCDI-C8/p-Si structure were compared with those of other organic/p-Si structures (Table 3). In order to examine the effect of series resistance (R_S) in diodes, the values of R_S, BH and *n* were calculated by using modified Norde functions and Cheung's method, which are the most common methods. The C-V measures of the diodes were made at various frequencies and room temperatures. Diffusion potential (V_d), barrier height BH ($\phi_b(C-V)$) from C-V and free carrier concentration (N_A) values were calculated from the C $^{-2}$ -V graphs of the diodes. Photovoltaic parameters and light sensitivity were determined by taking current-voltage measures of both C0 and interlayer C1 diodes at room temperature and under illumination (100 mW/cm^2). The C1 heterojunction diode showed much better photovoltaic behavior with a photosensitivity value of 1418.7 compared to C0 with a photosensitivity value of 48.2. Therefore, PTCDI-C8 is a suitable candidate for optoelectronic devices, and the C1 heterojunction diode can be considered as a photodiode or photosensor in optoelectronic applications.

Table 3. *The parameters of C0 and C1 diodes obtained from the C-V characteristics*

Devices	Junction parameters			
	n	**Φ_b (eV)**	***I_{SC} (µA)***	***V_{OC} (mV)***
This study	2.10	0.74	1.91	320
Al/azure/p-Si [48]	1.15	0.64	26.5	134
Al/PyMIs/p-Si [45]	2.51	0.77	13.8	320
Al/p-Si/Coumarin: TiO2%5 [49]	2.66	0.76	5.32	310
Au/BOD-Dim/n-Si [46]	2.66	0.91	0.36	150
Au/PYR(G)/p-Si [39]	2.70	0.83	180	500

Al/PVO-Cu2Te/p-Si [31]	1.85	0.69	-	-
Al/1PA2N/p-Si [47]	1.78	0.89	0.017	130

Conflict of Interest

The authors declare that they have no conflict of interest regarding this article.

Statement of Research and Publication Ethics

The authors declare that this study complies with research and publication ethics.

References

[1] Gündüz, B., Kurban, M. (2018). Photonic, spectroscopic properties and electronic structure of PTCDI-C8 organic nanostructure. *Vibrational Spectroscopy*, 96, 46–51.

[2] Bedeloğlu, A., Demir, A., Bozkurt, Y., Sariciftci, N.S. (2010). Photovoltaic properties of polymer based organic solar cells adapted for non-transparent substrates. *Renewable Energy,* 35, 2301-2306.

[3] Zafer, C., Kus, M., Turkmen, G., Dincalp, H., Demic, S., Kuband, B., Teoman, Y., Icli, S. (2007). New perylene derivative dyes for dye-sensitized solar cells. *Solar Energy Materials & Solar Cells*, 91, 427–431.

[4] Peumans, P., Uchida, S., Forrest, S.R. (2003). Efficient bulk heterojunction photovoltaic cells using smallmolecular-weight organic thin films. *Nature*, 425, 158-162.

[5] Fana, H., Shia, W., Yub, X., Yu, J. (2016). High performance nitrogen dioxide sensor based on organic field-effect transistor utilizing ultrathin CuPc/PTCDI-C8 heterojunction. *Synthetic Metals*, 211, 161–166.

[6] Kucinska, M., Frac, I., Ulanski, J., Makowski, T., Nosal, A., Gazicki-Lipman, M. (2019). The role of surface morphology in a performance of top-gate OFETs prepared from a solution processable derivative of perylene bisimide. *Synthetic Metals,* 250, 12-19.

[7] Welford, A., Maniam, S., Ganna, E., Jiaoa, X., Thomsen, L., Langfordd, S.J., McNeill, C.R. (2019). Influence of alkyl side-chain type and length on the thin film microstructure and OFET performance of naphthalene diimide-based organic semiconductors. *Organic Electronics*, 75, 10537.

[8] Das, A.K., Mandal, R., Mandal, D.K. (2022). The current transport mechanism of Al/Beetroot/Cu used as an organic semiconductor Schottky diode is superior than natural dye-based thin film devices. *Microelectronic Engineering*, 261, 111816.

[9] Hendi, A.A., Al Orainy, R.H. (2014). Rectifying properties of TIPS-pentacene:rhodamine blend organic semiconductor-on-p-silicon diodes. *Synthetic Metals*, 193, 31–34.

[10] Barış, B. (2013). Frequency dependent dielectric properties in Schottky diodes based on rubrene organic semiconductor. *Physica E*, 54, 171–176.

[11] He, J., Liang, B., Yan, X., Liu, F., Wang, J., Yang, Y., and et al. (2021). A TPA-DCPP organic semiconductor film-based room temperature NH3 sensor for insight into the sensing properties. *Sensors & Actuators: B. Chemical*, 327, 128940.

[12] Aziz, F., Sayyad, M.H., Sulaiman, K., Majlis, B.H., Karimov, K.S., Ahmad, Z., and Sugandi, G. (2012). Corrigendum: Influence of humidity conditions on the capacitive and resistive response of an Al/VOPc/Pt co-planar humidity sensor. *Meas. Sci. Technol.*, 23, 069501.

[13] Huang, Y., Fu, F., Zouc, W., and Zhang, F. (2012). Probing the effect of substituted groups on sensory properties based on single-crystalline micro/nanostructures of perylenediimide dyes. *New J. Chem.*, 36, 1080–1084.

[14] Chae, H., Hwang, S., Kwon, J.E., Pham, Q.B., Kim, S.J., Lee, W.H., Kim, B.G. (2021). Comparative study on the intrinsic NO2 gas sensing capability of triarylamine-based amorphous organic semiconductors. *Dyes and Pigments*, 186, 109017.

[15] Abhijith, T., Ameen, M.Y., and Reddy, V.S. (2015). Synthesis of PTCDI-C8 one dimensional nanostructures for photovoltaic applications. *IOP Conf. Series: Materials Science and Engineering*, 73, 012052.

[16] Erdoğan, E. and Gündüz, B. (2106). Controlling of the Optical Properties of the Solutions of the PTCDI-C8 Organic Semiconductor. *Electronic Materials Letters*, 12, 773–778.

[17] Rahimi, R. and Korakakis, D. (2009). Organic thin film transistors based on Pentacene and PTCDI as the active layer and LiF as the insulating layer. *MRS Online Proceedings Library*, 1197, 38–43.

[18] Balakrishnan, K., Datar, A., Naddo, T., Huang, J., Oitker, R., Yen, M., Zhao, J., and Zang, L. (2006). Effect of Side-Chain Substituents on Self-Assembly of Perylene Diimide Molecules: Morphology Control. *J. AM. CHEM. SOC.*, 128, 7390-7398.

[19] Nguyen, M., Turak, A.Z., Maye, F., Heidkamp, J., Wrachtrup, J., Dosch, H. (2010). Island size effects in organic optoelectronic devices. Proc. SPIE 7722, *Organic Photonics IV*, 77221O.

[20] Huang, C, Barlow, S., and Marder, S.R. (2011). Perylene-3,4,9,10-tetracarboxylic Acid Diimides: Synthesis, Physical Properties, and Use in Organic Electronics. *J. Org. Chem.*, 76, 2386–2407.

[21] Karak, S., Reddy, V.S., Ray, S.K., Dhar, A. (2009). Organic photovoltaic devices based on pentacene/N, N0 -dioctyl-3,4,9,10- perylenedicarboximide heterojunctions. *Organic Electronics*, 10, 1006–1010.

[22] Güllü, Ö. (2022). Dielectric spectroscopy studies on AL/p-Si photovoltaic diodes with Coomassie Brilliant Blue G-250. *Applied Physics A*, 128, 7, 587.

[23] Barıs¸ B., Yüksel, Ö.F., Tugluoglu, N., Karadeniz, S. (2013). Double barrier heights in 5,6,11,12-tetraphenylnaphthacene (rubrene) based organic Schottky diode. *Synthetic Metals*, 180, 38–42.

[24] Forrest, S.R., Kaplan, M. L., Schmidt, P. H. (1984). Organic-on-inorganic semiconductor contact barrier diodes. I. Theory with applications to organic thin films and prototype devices. *Journal of Applied Physics*, 55, 1492.

[25] Campbell, I. H., Rubin, S., Zawodzinski, T. A., Kress, J. D., Martin, R. L., Smith, D. L., Barashkov, N. N., Ferraris, J. P. (1996). Controlling Schottky energy barriers in organic electronic devices using self-assembled monolayers. *Phys. Rev. B*, 54, R14321(R).

[26] Huang, W.C., Lin, T.C., Horng, C.T., Chen, C.C. (2013). Barrier heights engineering of Al/p-Si Schottky contact by a thin organic interlayer. *Microelectronic Engineering*, 107, 200–204.

[27] Stella, M., Villar, F., Rojas, F.E., Pirriera, M.D., Voz, C., Puigdollers, J., Asensi, J.M., Andreu, J., and Bertomeu, J. "Optical and Morphological Characterization of PTCDI-C13", *MRS Online Proceedings Library (OPL), 1091: Symposium AA – Conjugated Organic Materials–Synthesis, Structure, Device and Applications*, 1091-AA05-40, 2008.

[28] Tung, R. T. (1992). Electron transport at metal-semiconductor interfaces: General theory. *Phys. Rev. B*, 45, 13509.

[29] Güllü, Ö., Kılıçoğlu, T., Türüt, A. (2010). Electronic properties of the metal/organic interlayer/inorganic semiconductor sandwich device. *Journal of Physics and Chemistry of Solids*, 71, 351-356.

[30] Rhoderick E.H. and Williams R.H. (1988). Metal-semiconductor contacts. Oxford science publication, 2nd edn., Oxford.

[31] Marıl, E. (2021). The effect of (PVP-Cu2Te) organic interlayer on the electrical parameters of Al/p-Si Schottky barrier diodes (SBDs) at room temperature. *Physica B*, 604, 412732.

[32] Karadeniz, S., Barıs¸ B., Yüksel, Ö.F., Tugluoglu, N. (2013). Analysis of electrical properties of Al/p-Si Schottky contacts with and without rubrene layer. *Synthetic Metals*, 168, 16–22.

[33] Imer, A.G., Korkut, A., Farooq, W. A., Dere, A., Atif, M., Atif, H., Karabulut, A. (2019). Interface controlling study of silicon based Schottky diode by organic layer. *Journal of Materials Science: Materials in Electronics*, 30, 19239–19246.

[34] Güllü, Ö., Türüt, A. (2010). Electrical analysis of organic dye-based MIS Schottky contacts. *Microelectronic Engineering*, 87, 12, 2482-2487.

[35] Cheung, S.K., Cheung, N.W. (1986). Extraction of Schottky diode parameters from forward current-voltage characteristics. *Appl. Phys. Lett.*, 49, 85–87.

[36] Norde, H. (1979). A modified forward I-V plot for Schottky diodes with high series resistance. *J. Appl. Phys*, 50, 5052–5053.

[37] Bohlin, K.E. (1986). Generalized Norde plot including determination of the ideality factor. *Journal of Applied Physics*, 60, 1223.

[38] Aydoğan, Ş., Sağlam, M., Türüt, A., Onganer, Y. (2009). Series resistance determination of Au/Polypyrrole/p-Si/Al structure by current–voltage measurements at low temperatures. *Materials Science and Engineering C*, 29, 1486–1490.

[39] Farag, A.A.M., Soliman, H.S., Atta, A.A. (2012). Analysis of dark and photovoltaic characteristics of Au/Pyronine G(Y)/p-Si/Al heterojunction. *Synthetic Metals*, 161, 23–24, 2759-2764.

[40] Sze, S.M. (1981). Physics of Semiconductor Devices. Wiley, second ed., New York.

[41] Özaydin, C., Tombak, A., Boğa, M., Kiliçoğlu, T. (2015). Optical, Electrical and Photoelectrical Properties of Quercetin Co(II) Complex/n-Si Organic-Inorganic Hybrid Device, *Middle East Journal of Science(MEJS)*, 1, 15–27.

[42] Gunduz, B., Yahia, I.S., Yakuphanoglu, F. (2012). Electrical and photoconductivity properties of p-Si/P3HT/Al and p-Si/P3HT: MEH-PPV/Al organic devices: Comparison study. *Microelectronic Engineering*, 98, 41–57.

[43] Yakuphanoglu, F., Farooq, W.A. (2011). Flexible pentacene organic field-effect phototransistor. *Synthetic Metals* 161, 79–383.

[44] Yakuphanoglu, F., Senkal, B.F. (2008). Electrical characterization of the polyaniline including boron/p-type silicon structure for optical sensor applications. *Synthetic Metals*, 158, 821–825.

[45] Tezcan, A.O., Oruç, P., Tuğluoğlu, N., Eymur, S. (2023). Photosensitive properties of Schottky type photodiodes prepared by spin coating of isoniazid Schiff base thin film on p-Si. *Optical and Quantum Electronics*, 56:989.

[46] Şahin, M.F., Taşcı, E., Emrullahoğlu, M., Gökçe, H., Tuğluoğlu, N., Eymur, S. (2021). Electrical, photodiode, and DFT studies of newly synthesized π-conjugated BODIPY dye-based Au/BOD-Dim/n-Si device. Physica B, 614, 413029.

[47] Sunkur, M., Gullu, O. (2023). Spectroscopic analysis and device application of molecular organic dye layer in the Al/p-Si MIS contacts. Journal of Physics and Chemistry of Solids, 178, 111360.

[48] Orak, İ., Turut, A., Toprak, M. (2015). The comparison of electrical characterizations and photovoltaic performance of Al/p-Si and Al/Azure C/p-Si junctions devices. *Synthetic Metals*, 200, 66-73.

[49] Aslan, F., Esen, H., Yakuphanoglu, F. (2019). Al/P-Si/Coumarin:TiO2/Al Organic-Inorganic Hybrid Photodiodes: Investigation of Electrical and Structural Properties. *Siliicon*, 12, 2149-2164.